

Microphotoluminescence studies of single InGaN quantum dots

R A Taylor, J W Robinson, J H Rice, J H Na, K H Lee, M J Holmes

Department of Physics, University of Oxford, Parks Road, Oxford, OX1 3PU, UK

R A Oliver, M J Kappers, C J Humphreys

Department of Materials, University of Cambridge, Pembroke Street, Cambridge, CB2 3QZ, UK

Y Arakawa

Research Center for Advanced Science and Technology, University of Tokyo, Komaba, Meguro-ku, Tokyo 153-0041, Japan

Main contact email address: *r.taylor1@physics.ox.ac.uk*

Introduction

In quantum dots (QDs), electrons and holes are confined in all three spatial dimensions. These structures therefore possess discrete energy levels where each level can accommodate just two electrons or holes of different spin due to the Pauli Exclusion Principle (analogous to an atom). QDs exhibit interesting fundamental physics, and have been used in optoelectronic applications such as laser diodes. An understanding of the basic optical properties of individual QDs such as exciton recombination dynamics and the behaviour of exciton complexes is essential to exploit fully the potential of QDs for use in classical and quantum optoelectronics.

In III-arsenide QD systems, microphotoluminescence (μ PL) spectroscopy has been used to study fundamental exciton complexes in single QDs. In reference¹, exciton (X) and biexciton (XX) states in an AlInAs QD were characterized, and in reference² the dynamics of the X and XX in a single InAs QD were studied using time-resolved μ PL spectroscopy. The decay traces revealed a coupling between the emission from the X and XX.

Other work characterizing the Quantum Confined Stark Effect (QCSE) in single self-assembled QDs has shown that the application of an external electric field in the lateral direction permits control of the exciton wavefunction. Studies on GaAs QDs have demonstrated that a lateral electric field produces an energy shift with linear and quadratic components, arising respectively from permanent dipole moment and polarizability contributions³. This is in contrast to single CdSe QDs, for which only a quadratic energy shift with electric field is observed, the permanent dipole moment contribution being negligible⁴.

The properties of QDs in III-nitride material systems^{5, 6} differ from those in conventional III-arsenide and II-selenide materials due to the strong piezoelectric fields and high exciton binding energies. μ PL spectroscopy has been used to probe single InGaN QDs^{5, 6}. The dynamics of exciton recombination in single InGaN QDs have been investigated⁷, but the dynamics of exciton complexes have not previously been studied. Moreover, the effect of a lateral electric field upon exciton recombination in single InGaN QDs has not been investigated.

In this report, two sets of experimental results are discussed. We first present a study of the dynamics of X and XX recombination in a single InGaN QD. Time-resolved measurements show that the recombination lifetime of the XX (~ 1.4 ns) is longer than that of the X (~ 1.0 ns). In the second set of experimental results, the effect of applying an external lateral electric field to a single InGaN QD is studied. The field-dependent shift as expressed by $\Delta E(F) = \mu F - \alpha F^2$ is found to possess non-zero linear and quadratic contributions.

Experimental

The two samples were grown by metal-organic vapour phase epitaxy (MOVPE) using two different methods. In Sample A⁵, the growth of a strained InGaN epilayer gave rise to the spontaneous formation of nanostructures (probably via the well-

known Stranski–Krastanov growth mode). In Sample B⁶, nanostructure formation was induced by annealing a flat InGaN epilayer in N_2 . In both cases, the InGaN layer was overgrown with a GaN cap, and a 100-nm-thick Al layer was later evaporated onto the sample surface. In the case of Sample A, a mask pattern was fabricated using electron-beam lithography together with reactive ion etching using $SiCl_4$. Square apertures were produced with side length varying from 2 μ m to 100 nm, together with markers to indicate their position and size. In the case of Sample B, an electrode pattern (consisting of a pair of Al electrodes with a separation of 1 μ m) was fabricated.

Spatially-resolved PL measurements were made using a temperature-controlled microscope cryostat and a *Coherent* “MIRA” Ti:Sapphire laser (150 fs pulse width), either frequency-doubled to 400 nm or frequency-tripled to 266 nm. The laser was focused through a 36 \times microscope objective lens to a spot size of ~ 2 μ m, the spot being aligned with features on the sample surface using a CCD camera. The PL was collected by the same microscope objective lens and time-integrated spectra were recorded using a cooled CCD camera mounted on a 0.30 m monochromator, which was equipped with a 1200 grooves/mm grating giving a spectral resolution of ~ 0.7 meV. Time-resolved PL measurements were performed using the same monochromator (the PL being directed out of a different exit port using a flipper mirror), together with a time-correlated single photon counting detection system based on a fast photomultiplier tube (PMT) with a time resolution of 150 ps.

Time-resolved study of exciton and biexciton transitions

Time-integrated μ PL spectra from a single InGaN QD in Sample A were recorded at 4.2 K. Figure 1(a) displays μ PL spectra at three excitation power densities: (i) 3×10^3 Wcm^{-2} , (ii) 8×10^2 Wcm^{-2} and (iii) 8×10^1 Wcm^{-2} . The spectrum recorded at 3×10^3 Wcm^{-2} shows two peaks at 2.825 eV and 2.866 eV (assigned to X and XX transitions respectively). Figure 1(b) shows the peak intensities of the X and XX lines as a function of power density. Calculation of the gradient for X showed linear power dependence, with an exponent of 0.96 ± 0.2 , while the XX line showed quadratic power dependence, with an exponent of 2.02 ± 0.4 . These gradients match the expected values for X and XX emission lines (i.e. 1.0 and 2.0 respectively).

To confirm these peak assignments, calculations of the X and XX wavefunctions and energies were performed using a one-band Hamiltonian within the Hartree approximation, solved with an iterative self-consistent finite difference method⁸. Using the QD dimensions and composition given in reference⁵, calculations using an In content of 7% gave an X energy of 2.819 eV and an X – XX splitting of 51 meV, which compare well with the experimentally observed 2.825 eV X energy and 41 meV X – XX splitting.

Figure 2(a) and (b) show background-subtracted⁷ time-resolved decay traces from the XX and X shown in Figure 1. In Figure 2(a), the XX trace shows a mono-exponential decay (lifetime ~ 1.4 ns) with no rounding at the peak. In Figure 2(b), the X trace (lifetime ~ 1.0 ns), by contrast, shows a rounding effect,

with the peak intensity also being delayed relative to the XX trace by ~ 1.0 ns. Both the delay and the rounding are attributed to the refilling of X states as XX states decay radiatively via the process $XX \rightarrow X + \text{photon}$, as observed previously in III-arsenide²⁾ QD systems. Figure 2(c) shows an X decay trace from a different single InGaN QD⁷⁾, for which no XX line was observed at the power density used. In contrast to the X decay trace seen in Figure 2(b), this X trace shows no rounding: the decay is found to be mono-exponential with a lifetime of 1.07 ns. This is expected as there is no XX state to cause refilling of the population of the X state in this case.

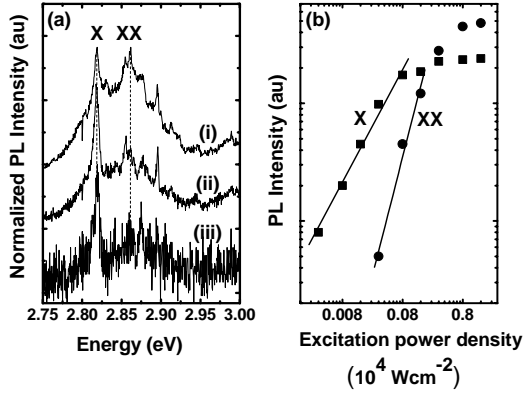


Figure 1. (a) μ PL spectra at a variety of power densities. (b) Dependence of the PL intensity on the power density.

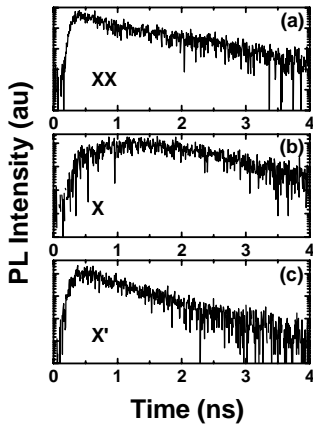


Figure 2. Time-resolved μ PL from (a) the XX and (b) the X in a single InGaN QD. (c) X decay from a different QD for which no XX was observed at the excitation power density used.

Effect of an external electric field

Figure 3(a) shows a series of spatially-resolved μ PL spectra from a single InGaN QD in Sample B, recorded at 4.2 K with increasing electric field (applied in the lateral direction using electrodes placed on the sample surface⁹⁾). The PL peak redshifts and declines in intensity as the applied voltage is increased from 0 V to 10 V. Figure 3(b) plots the relative peak intensity and the peak shift as a function of voltage. At 10 V, a peak shift of $\Delta E = 5.4$ meV to lower energy is found. This is in line with previous measurements on epitaxial III-arsenide QDs³⁾ and II-selenide QDs⁴⁾, which showed redshifts in exciton recombination energies of up to $\Delta E = 1.1$ meV. This behaviour can be readily understood in terms of the QCSE. The electric field forces the electron and hole to opposite sides of the QD and band tilting leads to a reduction in the bandgap, and thus to a redshift of the PL.

An external electric field F applied to a single QD is expected to produce a shift $\Delta E(F)$ in the exciton recombination energy which consists of both linear and quadratic terms. This shift arises from the QCSE and may be expressed as:

$$\Delta E(F) = \mu F - \alpha F^2, \quad (1)$$

where μ and α are respectively the components of the permanent dipole moment and the polarizability in the direction of the electric field. A fit was made to the plot in Figure 3(b) using equation (1), yielding values of $\mu = -1.52 \times 10^{-28}$ C m and $\alpha = -2.32 \times 10^{-35}$ J V⁻² m².

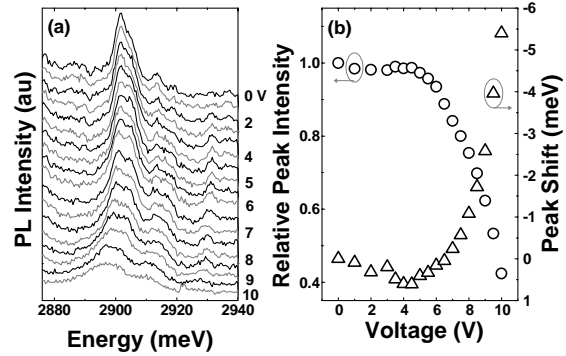


Figure 3. (a) μ PL spectra with increasing externally-applied lateral electric field, and (b) relative peak intensity and peak shift as a function of applied voltage.

Conclusion

Time-resolved μ PL studies of X and XX transitions in a single InGaN QD have shown a rounding of the X decay trace and a delay relative to the XX trace, attributed to refilling of the X population by XX decays. Additionally, the application of an external electric field in the lateral direction to a single InGaN QD is found to cause a redshift in the exciton recombination energy of more than 5 meV, together with a reduction in the PL intensity. The field dependence as expressed by $E(F) = \mu F - \alpha F^2$ is found to possess non-zero linear and quadratic contributions, indicating that the component of the permanent dipole moment in the lateral direction is not insignificant.

Acknowledgements

We gratefully acknowledge D G Hasko and S Yasin for help with sample masking. This work was supported by the Foresight LINK Award *Nanoelectronics at the Quantum Edge* (www.nanotech.org), by EPSRC GR/R66029/01 and by Hitachi Cambridge Laboratory.

References

1. K Hinzer, *et al.*, Phys. Rev. B, **63** 075314, (2001)
2. R M Thompson, *et al.*, Phys. Rev. B, **64** 201302, (2001)
3. W Heller, *et al.*, Phys. Rev. B, **57** 6270, (1998)
4. J Seufert, *et al.*, Appl. Phys. Lett., **79** 1033, (2001)
5. O Moriwaki, *et al.*, Appl. Phys. Lett., **76** 2361, (2000)
6. R A Oliver, *et al.*, Appl. Phys. Lett., **83** 755, (2003)
7. J W Robinson, *et al.*, Appl. Phys. Lett., **83** 2674, (2003)
8. J H Rice, *et al.*, Nanotech. (submitted)
9. J W Robinson, *et al.*, Appl. Phys. Lett., **86** 213103, (2005)